Assessing the Chemical Speciation during CO2 Absorption by Aqueous Amines Using in Situ FTIR

ARTICLE *in* INDUSTRIAL & ENGINEERING CHEMISTRY RESEARCH · OCTOBER 2012

Impact Factor: 2.59 · DOI: 10.1021/ie302056f

2 AUTHORS:

Gilles Richner
Bern University of Applied Sciences
12 PUBLICATIONS **94** CITATIONS
SEE PROFILE

Graeme Puxty
The Commonwealth Scientific and Industrial …
65 PUBLICATIONS **1,183** CITATIONS
SEE PROFILE

I&EC research
Industrial & Engineering Chemistry Research

Article

pubs.acs.org/IECR

Assessing the Chemical Speciation during CO_2 Absorption by Aqueous Amines Using *in Situ* FTIR

Gilles Richner* and Graeme Puxty

CSIRO Energy Technology, P.O. Box 330, Newcastle, NSW 2300, Australia

ABSTRACT: During amine scrubbing of CO_2 from flue gas, carbamate and bicarbonate species are formed, the amount of which is directly related to the process performance. In this study we present a fast calibration-free spectroscopic technique for determining the speciation of CO_2−H_2O−alkanolamine systems and in turn the amine protonation and carbamate thermodynamic equilibrium constants. The method is based on *in situ* infrared monitoring of the liquid phase during CO_2 absorption by an aqueous amine solution in a stirred vessel, combined with mathematical hard modeling of the reaction mechanism. The species concentrations are calculated by fitting of a thermodynamic model to multivariate spectroscopic measurements using nonlinear regression. Successful applications include the determination of the amine protonation and carbamate equilibrium constants of one primary (MEA), one secondary (DEA), and one sterically hindered primary (AMP) amine at 40 °C.

INTRODUCTION

CO_2 capture and sequestration (CCS) is of growing importance for striking a balance between the increasing global demand for energy and the need to mitigate greenhouse gas emissions. In CCS, CO_2 is separated from the other components of a flue gas at the emission source (e.g., coal-fired power station), compressed, and transported into a storage site. The most mature technique for capturing CO_2 from emissions sources is based on absorption into an aqueous amine solution in a temperature swing process. CO_2 chemically reacts with the amine solution at low temperature (typically 40 °C) and is regenerated at high temperature (e.g., 120 °C) as the reaction is thermally reversed.[1]

During the absorption phase, the reaction between CO_2 and the aqueous amine solution forms carbamate and/or bicarbonate. The amount of each product is directly related to the absorption rate and the energy requirement for absorbent regeneration. A precise characterization of the thermodynamic equilibrium of the CO_2−H_2O−alkanolamine system is paramount for process design and optimization.

During the early stage of process development, the performance of new amine-based absorbents is typically evaluated by measurements of the CO_2 absorption capacity and absorption rate.[2,3] While these measurements allow a fast screening of amines to identify outstanding candidates, they are lacking in providing species concentrations and thermodynamic behavior in solution.

To gain insight into the chemical equilibrium in solution, chemical speciation can be determined by spectrometric techniques. Online NMR (nuclear magnetic resonance) was successfully applied to determine speciation in several CO_2−H_2O−alkanolamine systems.[4,5] ^{1}H NMR in combination with UV−vis spectroscopy coupled to a stopped-flow reactor has allowed the rigorous description of the reaction mechanism and associated kinetic and thermodynamic parameters of CO_2 in aqueous MEA.[6,7]

Fourier transform infrared spectroscopy (FT-IR) is a reliable analytical technique widely used in chemistry for online reaction monitoring. Changes of a molecule's dipole moment due to molecular deformations are measurable in the mid-IR region (4000−400 cm^{-1}), allowing identification and quantification of many of the chemical compounds. Attenuated total reflectance (ATR) FT-IR measures changes occurring in a film a few micrometers thick in contact with a probe surface rather than in a sample cell, making this technique perfectly suited for *in situ* investigation with immersion probes.

Qualitative identification of amine, carbamate, and bicarbonate species during the absorption of CO_2 in aqueous solutions of monoethanolamine (MEA), 2-amino-2-methyl-1-propanol (AMP), methyldiethanolamine (MDEA),[9] and some heterocyclic amines[10] have been recently reported. Infrared monitoring also allows quantitative measurements according to the Beer−Lambert law (the absorbance changes linearly with species concentration). Determining speciation often relies on time-consuming calibration of pure components at different concentrations.[11] With CO_2−H_2O−alkanolamine systems, these calibrations are based on a single peak evaluation (e.g., the amplitude of the absorbance peak at a certain wavenumber that is due to one species only). The sum of individual contributions from multiple species (peak overlap) are not considered making such an evaluation inaccurate. For example, Archane et al.[12] observed that with aqueous diethanolamine (DEA), the height of the bicarbonate peak was not estimated with a sufficient accuracy (20% errors) as DEA and the protonated moiety $DEAH^+$ contribute to the absorbance in the same region of the spectra. Moreover, the molar absorptivity of the carbamate could not be calibrated.[8]

A partial least-squares (PLS) model is an alternative calibration technique for real-time performance monitoring. This method requires well-designed calibration and validation

Received: August 1, 2012
Revised: October 2, 2012
Accepted: October 4, 2012
Published: October 4, 2012

dx.doi.org/10.1021/ie302056f | *Ind. Eng. Chem. Res.* 2012, 51, 14317−14324

data sets at different gas pressures and amine concentrations. It has been successfully applied to FT-IR monitoring of the simultaneous absorption of CO_2 and SO_2 in a pilot plant.[13] Unsurprisingly, this method failed to provide accurate concentrations under conditions outside those covered by the data set.

In this study, we present a simple, fast, robust, and calibration-free method for determining the CO_2 loading, the speciation, and in turn the equilibrium constants of CO_2−H_2O−amine system based on *in situ* infrared monitoring of vapor−liquid−equilibrium (VLE) experiments combined with mathematical modeling of the reaction equilibrium. This method aims at minimizing the number of experiments required during the early stage of process development, while increasing the amount of information extracted (i.e., speciation, concentration, and equilibrium constants) compared to standard VLE experiments in the search for new CO_2 absorbents. First the absorbance bands observed during CO_2 absorption by MEA (primary amine), DEA (secondary amine), and AMP (sterically hindered primary amine) are rigorously assigned to characteristic vibration modes. Then, independently of the band assignments, the amine protonation and carbamate equilibrium constants are calculated by fitting a thermodynamic model to multivariate spectroscopic measurements using nonlinear regression.

EXPERIMENTAL SECTION

Materials. All the experiments were performed in a 150 mL custom-built high-pressure metal vessel (Parr Instruments) equipped with a pressure transducer, P_r (Swagelok) and a turbine impeller as depicted in Figure 1. The temperature of the

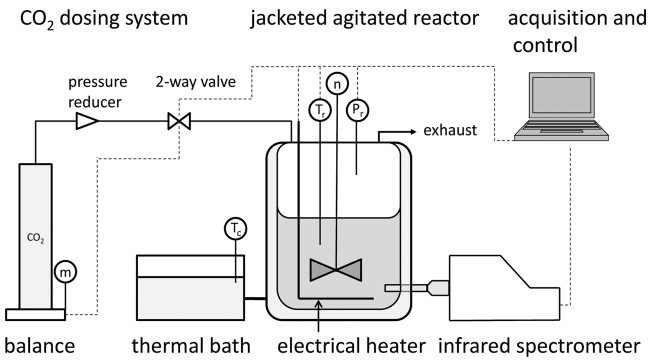

Figure 1. VLE apparatus with CO_2 dosing unit and infrared monitoring.

reactor content, T_r, was kept isothermal at 40 °C by a power compensation electrical heater (Watlow) dipping into the aqueous solution. The temperature of the cooling system, T_c, was set 5 deegrees below the reactor temperature. The mass of CO_2 dosed into the vessel was measured with a balance (PB4002-S, Mettler Toledo) from the mass loss, m, of the CO_2 gas reservoir.[2] Instrumental control and data acquisition was done with Labview software at a sampling rate of 1 Hz running on a personal computer.

The liquid phase was monitored with a 6 mm ATR-FT-IR DiComp immersion probe connected to an iC10 infrared spectrometer via a K-6 mirror conduit from Mettler-Toledo. The spectrometer collected two spectra/min (average of 16 scans) in the range of 650 cm^{-1} to 4000 cm^{-1} at a resolution of 2 cm^{-1}. The diamond sensor material absorbs in the 1950−2250 cm^{-1} region. All infrared backgrounds were taken at room temperature against N_2.

A typical experiment was performed as follows. The infrared probe was inserted from the flange of the empty vessel via a $^1/_4$ in. Swagelok connection. The vessel was purged with N_2 and the IR background measured. Then, 50 mL of 30 wt % aqueous amine (MEA (ReagentPlus, ≥99%), DEA (99%), AMP (BioUltra, ≥99.0%) purchased from Sigma-Aldrich and used as received) were added to the vessel. The vessel was then purged six times with 6 bar N_2 and heated to 40 °C under vigorous stirring, n, at 500 rpm. IR monitoring was started. Approximately 0.5 g of CO_2 (>99.9%, BOC Australia) was successively dosed into the vessel. Between each dosing the pressure was allowed to reach steady-state. All the experiments were performed at 40 °C as this is a standard temperature in PCC and, importantly, there is a wealth of thermodynamic constants available for comparison.

Data Treatment. Spectroscopic monitoring and model fitting is often used to determine reaction mechanisms and associated equilibrium[14] and/or kinetic[15] parameters. In this study a chemical model was fitted via nonlinear regression to multivariate spectroscopic IR data measured at equilibrium.

Chemical Model. A detailed reaction network including all reactions between monoamine, CO_2, and water comprises 11 species and 9 reactions/equilibrium.[6,7] In this study, a simplified equilibrium chemical model of the CO_2−H_2O−amine system was considered as follows:

$$H^+ + CO_3^{2-} \overset{K_1}{\rightleftharpoons} HCO_3^-$$

$$H^+ + HCO_3^- \overset{K_2}{\rightleftharpoons} CO_2(aq) + H_2O$$

$$H^+ + OH^- \overset{K_3}{\rightleftharpoons} H_2O$$

$$Am + H^+ \overset{K_4}{\rightleftharpoons} AmH^+$$

$$HCO_3^- + Am \overset{K_5}{\rightleftharpoons} AmCOO^- + H_2O$$

This model does not include protonation of the carbamate ($AmCOO^-$) to form carbamic acid (AmCOOH), and carbonic acid formation as there was no indication they were present at measurable concentrations. The model was however chosen to be as general as possible to cover the various behavior of different amines.

As concentrated amine solutions were considered in this work (30 wt %) the concentrations of ions can become large at high CO_2 loadings. As a consequence it was necessary to take into account nonideal behavior due to changes in the activity of charged species. In the calculation of the simultaneous equations the values of the equilibrium constants were corrected for ion activity by calculating activity coefficients (γ_i) with the form of the Debye−Hückel equation given below. More complex and accurate expressions for activity that include interaction parameters between ion pairs were considered but failed to give improved results. Furthermore, it was found in previous work[19] that the use of this equation (eq 1) adequately predicts equilibrium and absorption rate data for MEA, PZ, AMP, and MDEA and their mixtures at similar conditions to those used here. It was assumed that this was also the case for DEA, as it belongs to same class of compound (i.e., amine).

$$\log_{10}\gamma_i = \frac{Z_i^2 A\sqrt{I}}{1 + B\rho^{-1/2}\sqrt{I}} \quad (1)$$

dx.doi.org/10.1021/ie302056f | Ind. Eng. Chem. Res. 2012, 51, 14317−14324

where $A = (1.8248 \times 10^6)/(eT)^{3/2}$ (M) is the Debye–Hückel law slope,[20] $B = 1.5$ is an empirical constant ($kg^{1/2}/mol^{1/2}$),[21] ρ is the density of water (kg/dm^3),[22] I is the ionic strength (M), and Z_i is the charge of species i.

The equilibrium constants including the activity coefficients for the above mechanism are given by

$$K_1 = \frac{[HCO_3^-]}{[H^+][CO_3^{2-}]} \times \frac{\gamma_{HCO_3^-}}{\gamma_{H^+}\gamma_{CO_3^{2-}}} \quad (2)$$

$$K_2 = \frac{[CO_2(aq)]}{[H^+][HCO_3^-]} \times \frac{1}{\gamma_{H^+}\gamma_{HCO_3^-}} \quad (3)$$

$$K_3 = \frac{[H_2O]}{[H^+][OH^-]} \times \frac{1}{\gamma_{H^+}\gamma_{OH^-}} \quad (4)$$

$$K_4 = \frac{[AmH^+]}{[Am][H^+]} \quad (5)$$

$$K_5 = \frac{[AmCOO^-]}{[HCO_3^-][Am]} \quad (6)$$

Activity coefficients for ions with a same charge are equal when using the Debye–Hückel equation. Therefore, in K_4 and K_5, the activity coefficients cancel. However, this is not the case in K_1–K_3 used to calculate the concentration of HCO_3^- which then effects the concentration of Am and AmH^+.

The equilibrium constants K_1 to K_3 describe CO_2 interactions with water, and are thus independent of the amine. The values of these equilibrium constants have been taken from published data as given in Table 1. The values of the amine protonation and carbamate formation constants, K_4 and K_5, were determined by nonlinear regression as described below.

Table 1. Published Equilibrium Constants of the Reaction of CO_2 with Water

equilibrium constant	value	ref
log K_1	10.22	16
log K_2	6.30	17
log K_3	15.28	17

Four additional equations (eqs 7–10) can be written in terms of the CO_2 balance, amine balance, proton balance, and hydroxide balance:

$$[CO_2]_{total} = [CO_3^{2-}] + [HCO_3^-] + [CO_2(aq)] + [AmCOO^-] \quad (7)$$

$$[Am]_{total} = [Am] + [AmH^+] + [AmCOO^-] \quad (8)$$

$$[H^+]_{total} = [H^+] + [HCO_3^-] + 2[CO_2(aq)] + [AmH^+] + [H_2O] \quad (9)$$

$$[OH^-]_{total} = [OH^-] + [H_2O] \quad (10)$$

This results in a system of nine nonlinear simultaneous equations (eqs 2–10). Given the values for the equilibrium constants and total CO_2, amine, proton, and hydroxide concentrations, the system of equations was solved for the concentrations of all species using the Newton–Raphson method.[18]

CO_2 Loading. The total amount of CO_2 introduced into the reactor vessel was measured by mass. At equilibrium the amount of CO_2 in the gas phase, $n_{CO_2,g}$ (mol), was determined using the following gas law:

$$n_{CO_2,g} = Z \times \frac{(P_{tot} - P_{H_2O,vap} - P_{N_2}) \times V_g}{RT} \quad (11)$$

where Z is the CO_2 compressibility factor,[23] P_{tot} the total measured pressure (Pa), $P_{H_2O,vap}$ is the water vapor pressure (Pa), P_{N_2} is the N_2 partial pressure (Pa), V_g is the gas volume (m^3), R is the gas constant (J/mol K), and T the temperature (K). The total amount of CO_2 in the liquid phase was then determined by the difference between the total amount added, m, and that remaining in the gas phase, eq 11.

Nonlinear regression. Spectroscopic data can be represented in matrix form according to Beer–Lambert's law:

$$\mathbf{Y} = \mathbf{C} \times \mathbf{A} + \mathbf{R} \quad (12)$$

where $\mathbf{Y}$ ($np \times ny$) is the measured absorbance data at np partial pressures and ny wavenumbers, $\mathbf{C}$ ($np \times nc$) is the matrix of concentration profiles of nc absorbing chemical species, $\mathbf{A}$ ($nc \times ny$) is the matrix of molar absorptivities for the nc chemical species at the ny wavenumbers, and $\mathbf{R}$ ($np \times ny$) is a matrix of residuals or errors.

Given guesses for the values of K_4 and K_5 the matrix of concentration profiles, $\mathbf{C}$, can be calculated from the chemical model, as described above. The matrix of molar absorptivities, $\mathbf{A}$, can then be estimated by linear regression using the pseudoinverse of $\mathbf{C}$, $\mathbf{C}^+$:

$$\mathbf{A} = \mathbf{C}^+\mathbf{Y} \quad (13)$$

This allows calculation of the residuals matrix, $\mathbf{R}$:

$$\mathbf{R} = \mathbf{Y} - \mathbf{C}\mathbf{C}^+\mathbf{Y} \quad (14)$$

In an iterative process the magnitude of the sum of the squared error (ssq) of $\mathbf{R}$ was minimized by adjusting the values of K_4 and K_5 using nonlinear regression:

$$ssq(K_4, K_5) = \sum_{i=1}^{np}\sum_{j=1}^{ny} \mathbf{R}(i,j)^2$$

$$\min_{K_4,K_5 \in \mathbb{R}^+} ssq(K_4, K_5) \quad (15)$$

The Newton–Gauss–Levenberg/Marquardt method was used as described elsewhere.[15]

The number of degrees of freedom is defined as the number of experimental values minus the total number of optimized parameters and should be positive to avoid mathematical ambiguities.[18] The number of parameters includes the number of fitted equilibrium constants (K_4 and K_5) and fitted molar spectra of all absorbing chemical species ($nc \times ny$). Therefore, the number of measured spectra, np, corresponding to $np \times ny$ experimental data points, should be higher than the number of absorbing species, nc.

RESULTS AND DISCUSSION

The infrared spectra of aqueous MEA 30 wt %, DEA 30 wt %, and AMP 30 wt % were recorded under different CO_2 loadings. In the following section the different absorbance bands have been assigned to corresponding vibrational modes to the extent

dx.doi.org/10.1021/ie302056f | Ind. Eng. Chem. Res. 2012, 51, 14317–14324

possible, considering there is considerable overlapping of bands. Then, a mathematical method for the chemical speciation and determination of the equilibrium constants from the infrared spectra of CO_2-loaded amine solutions is presented.

Assignment of Infrared Bands. All the IR measurements were performed in aqueous solution. O−H stretching of H_2O strongly absorbs between 3200 and 3700 cm^{-1}. Because of hydrogen bonding, these peaks are particularly broad. N−H, C−H, and O−H stretching of aminoalcohol molecules also absorb in this region known as *"the hydrogen stretching region"*. It is difficult to distinguish between these different contributions and the water peak dominates. As a consequence the wavenumber region from 3000 cm^{-1} to 4000 cm^{-1} did not provide useful information.

The spectra of the amines prior to CO_2 are given in Figure 2. The primary amines (MEA and AMP) show characteristic vibration modes at 1645 cm^{-1} and 1600 cm^{-1} (N−H rocking), 955 cm^{-1} (C−N−H out-of-plane wagging and C−NH_2 twisting, 914 cm^{-1} for AMP), in agreement with current literature.[24,25] In addition there are C−N and C−O stretching modes at 1076 cm^{-1} and 1024 cm^{-1}, respectively. For AMP, these two bands are strongly overlapping at around 1043 cm^{-1}.

Significant contribution from $-CH_2$, $-CH_3$, and C−C stretching of AMP absorb in the 1300 cm^{-1} region. This complexity and the overlapping of bands make it difficult to identify the individual vibrational modes. The main peaks at 1475 cm^{-1} and 1371 cm^{-1} are probably due to $-CH_3$ asymmetric and symmetric rocking.[25]

For DEA, C−O, and C−N stretching absorb at 1048 cm^{-1} and 1123 cm^{-1}, respectively. The latter is a characteristic asymmetric stretch as DEA is a secondary amine. The shoulder at 1069 cm^{-1} is probably due to the second C−N stretching mode. DEA should also show an N−H bend around 1650 cm^{-1} but this is strongly overlapping with the H_2O spectrum.[25] The band at 1460 cm^{-1} is unaffected by pH and thus is likely to be out-of-plane C−H vibration (wagging, twisting) (Figure 2b).

The specific bands of protonated amines were identified by acidification of the aqueous amine solutions with 37 wt % HCl until the pH reached approximately 1. For primary amines, Figures 2a,c, the bands at 1518 cm^{-1} and 1634 cm^{-1} are due to symmetric and asymmetric NH_3^+ scissoring (1526 cm^{-1} and 1636 cm^{-1} for AMP). C−N and C−O stretchings shift from 1076 to 1069 cm^{-1} and 1024 to 1013 cm^{-1}, respectively, as MEA protonates (in AMP, from 1043 to 1074 cm^{-1} and from 1043 to 1050 cm^{-1}). The protonation of DEA results in O−H and C−N peaks shifting from 1048 to 1033 cm^{-1} and from 1123 to 1097 cm^{-1}, respectively.

Carbonate and bicarbonate adsorption frequencies were assigned by monitoring CO_2 absorption by 1 M NaOH solution. The resulting spectra are shown in Figure 3. At low CO_2 loading carbonate is the most abundant species, with a typical absorption peak at 1388 cm^{-1} corresponding to the doubly degenerate stretching.[26] At higher CO_2 loading, as the pH decreases, the bicarbonate species dominates, showing peaks at 1360 cm^{-1} ($-CO_2^-$ symmetric stretching) and at 1298 cm^{-1} (C−OH bending).[27] The weak band at 1000 cm^{-1} is due to C−OH stretching.

Dissolved CO_2 showed an absorption peak at 2343 cm^{-1} due to asymmetric stretching[26] (Figure 3). This peak is located in a wavenumber range where no other peak occurs and has been previously used for evaluating the molecular CO_2 concentration.[26,28] However, in amine solutions, this absorbance is weak below 50 kPa CO_2. This wavenumber is also close to the ATR sensor absorption range.[9] This peak should therefore be used with caution for determining the concentration of dissolved CO_2.

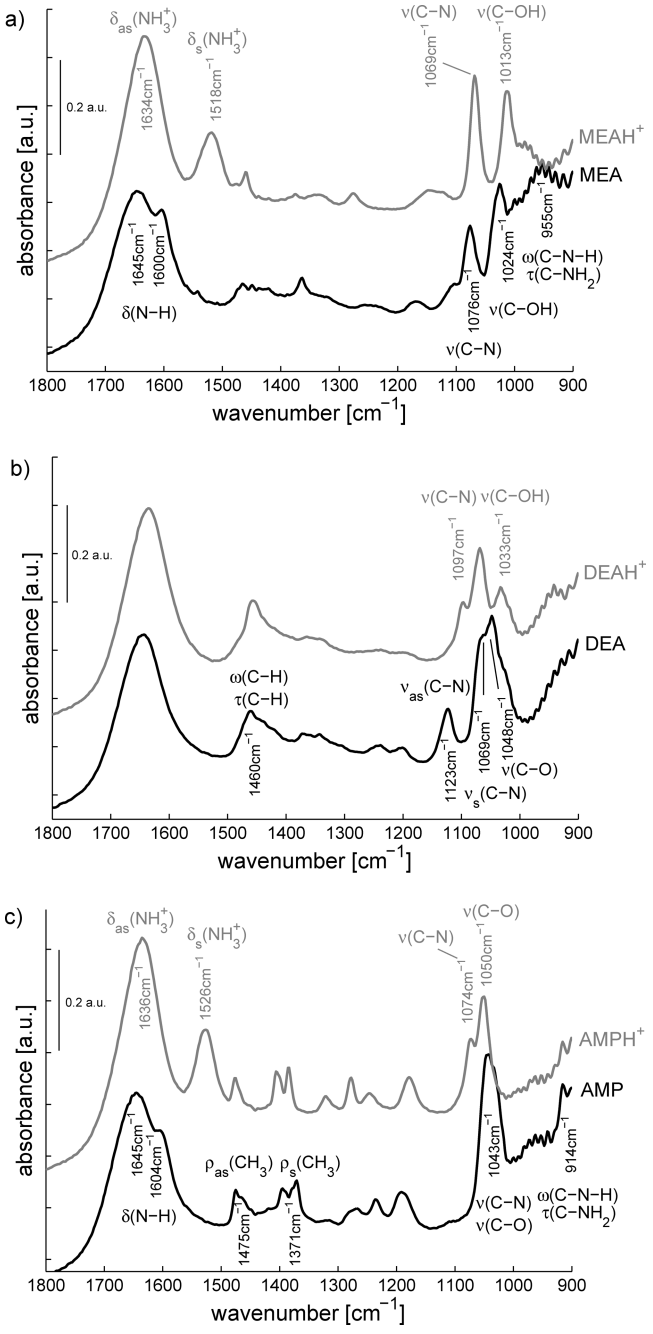

Figure 2. Infrared spectra of the liquid phase of 30 wt % aqueous amine (black line) and protonated amine (pH≈1, gray line) a) MEA, b) DEA, and c) AMP. The wavenumber regions from 650 cm^{-1} to 900 cm^{-1} and from 1800 cm^{-1} to 4000 cm^{-1} do not provide useful information.

Spectra of aqueous MEA at different CO_2 loadings are given in Figure 4 a. Several peaks appear or shift due to the formation of carbamate and bicarbonate, the protonation of the amine group, and the dissolution of molecular CO_2. The major peaks have been highlighted by arrows: top head for an increasing peak height, bottom head for decreasing peak height, and double arrows for increasing and then decreasing peak height as CO_2 loading increases.

dx.doi.org/10.1021/ie302056f | *Ind. Eng. Chem. Res.* 2012, 51, 14317−14324

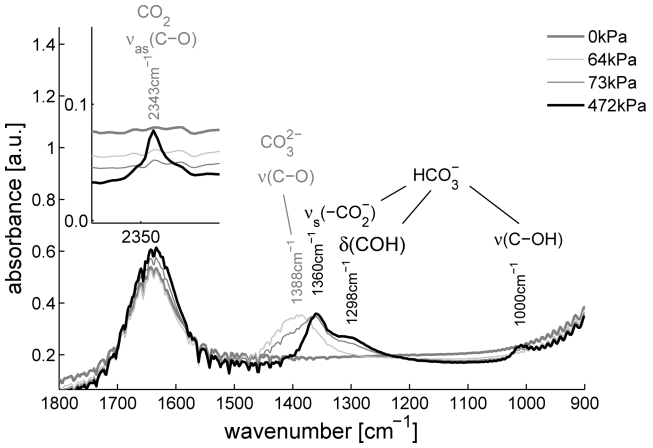

Figure 3. Infrared spectra of the liquid phase of 1 M NaOH under different CO_2 partial pressures, at 40 °C.

MEA-carbamate peaks were assigned to COO^- asymmetric and symmetric stretching at 1568 cm^{-1} and 1486 cm^{-1} respectively, and N-COO^- stretching vibration at 1322 cm^{-1}.[9,10,29,30]

Similarly to MEA, DEA carbamate absorbs at 1533 cm^{-1} (asymmetric stretching of COO^-),[28] at 1481 cm^{-1} (symmetric stretching of COO^-) as well as at 1296 cm^{-1} (stretching of N-COO^-). The peak at 1414 cm^{-1} increases and then decreases at high CO_2 content, and is likely to be carbamate.

In AMP, carbamate is not formed (or forms in negligible concentration) and all the peaks in Figure 4 c can be assigned to amine, protonated amine, and bicarbonate.

In this section, IR absorption bands have been assigned to the different species, namely H_2O, amine, carbonate, carbamate, as well as the protonated moieties. The complexity of infrared spectra due to the number of absorbing species makes it difficult to precisely assign all the absorption bands. Several bands are close to each other, very broad, and/or strongly overlapping. To help, reference spectra were recorded. For example, the acidification of aqueous amines allowed an assignment of the absorbance specific to the protonated moieties. CO_2 absorption in NaOH allowed identification of carbonate and bicarbonate contributions. However, the calibration of the IR extinction coefficients were difficult as peaks were close and may strongly overlap. For example, the typical band of bicarbonate at 1354 cm^{-1} is strongly overlapped by a carbamate (C–N) stretch at 1322 cm^{-1} as already mentioned elsewhere.[12]

Data Fitting. The new method proposed in this study does not require any knowledge nor calibration of the pure component spectra or even assignment of the absorption peaks. The method is based on a mathematical hard modeling of the different equilibria. The chemical reactions involved during the absorption of CO_2 in aqueous amine can be described with a general model described by a reaction network and a set of equations (eqs 2–10).

The reversible interactions of CO_2 with H_2O and OH^- to form carbonate and bicarbonate in aqueous solution are described by K_1 to K_3. These interactions are independent of the amine, and thus, due to the wealth of data available in literature, are not calculated in this study. K_4 and K_5 represent the equilibrium constants of amine protonation and carbamate formation. These equilibrium constants are fitted from the spectral data.

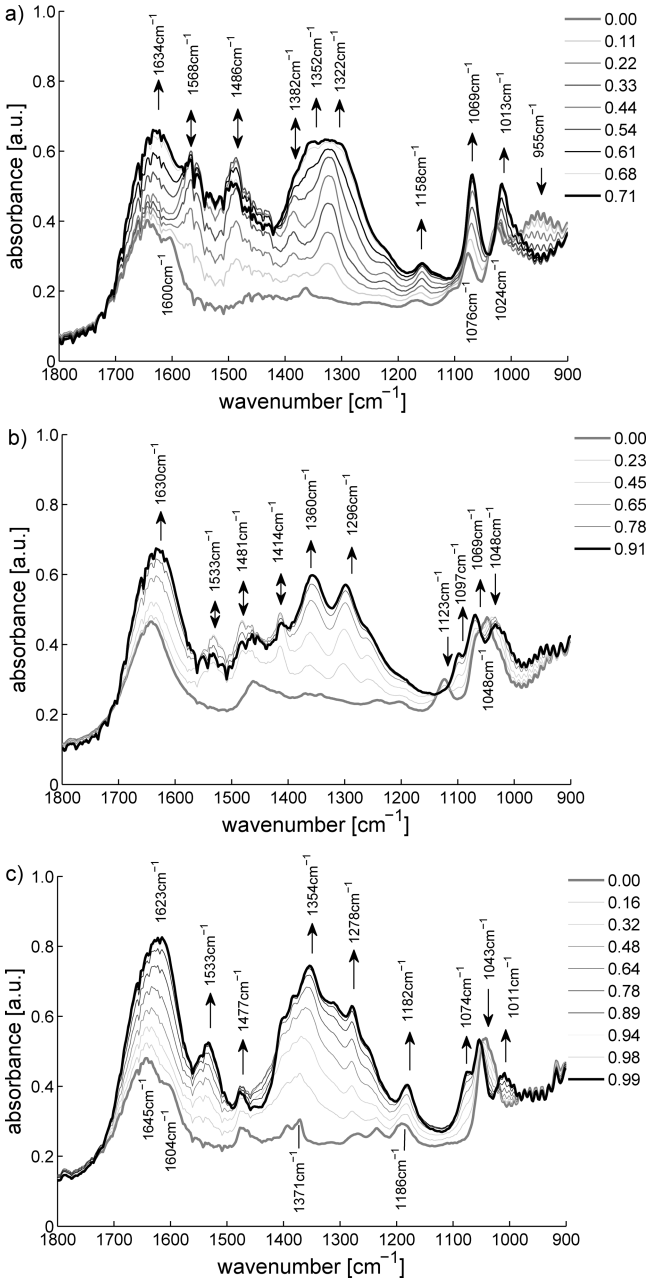

Figure 4. Infrared spectra of the liquid phase of 30 wt % aqueous amine under different CO_2 loadings, at 40 °C, (a) MEA, (b) DEA, and (c) AMP. The wavenumber regions from 650 cm^{-1} to 900 cm^{-1} and from 1800 cm^{-1} to 4000 cm^{-1} do not provide complementary information.

Data in the range 900–1800 cm^{-1} was used for fitting. HCO_3^-, Am, and $AmCOO^-$ were set as IR absorbing species. AmH^+ was set as nonabsorbing due to rank deficiency with HCO_3^- and $AmCOO^-$ (their concentrations are linearly dependent within the concentration range investigated here). For AMP the absorbing species were set to CO_3^{2-}, Am and HCO_3^-. The greater basicity of AMP meant that carbonate formed in an appreciable amount.

The fitted and measured absorbances at selected wavenumbers are plotted against CO_2 loading and allow evaluation of the quality of the fit (Figure 5). Clearly the agreement between the measured and model determined absorbance values is excellent.

dx.doi.org/10.1021/ie302056f | Ind. Eng. Chem. Res. 2012, 51, 14317–14324

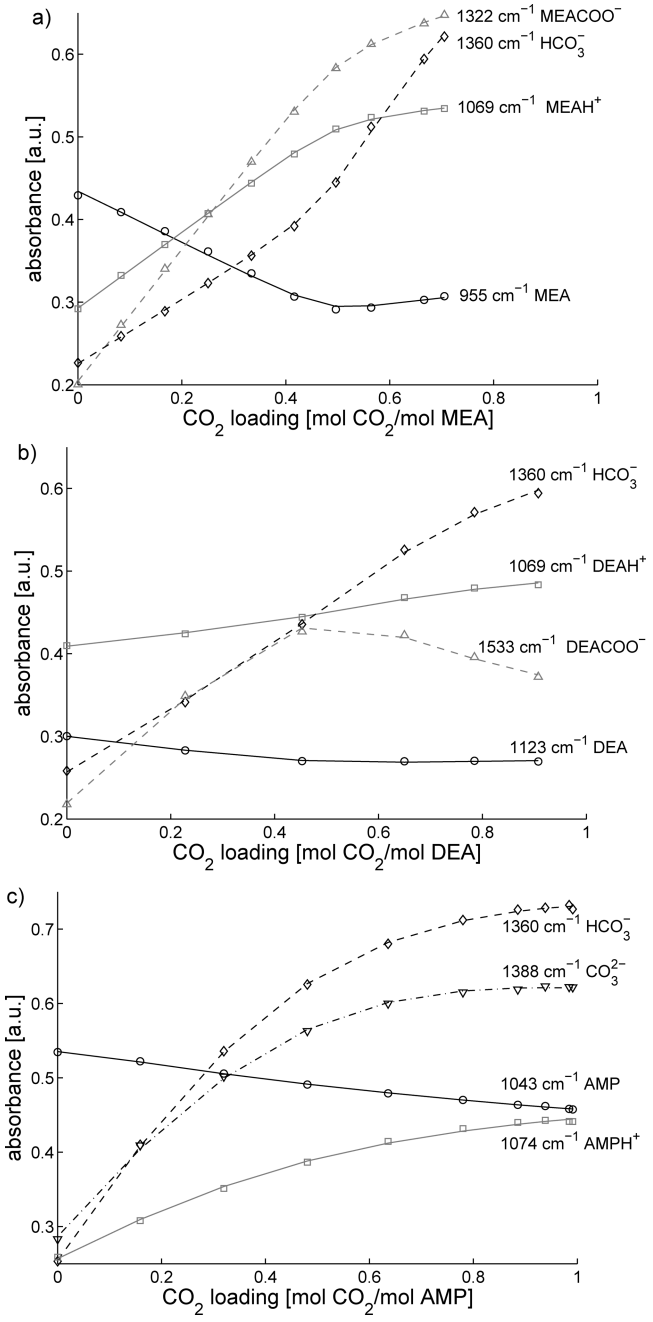

Figure 5. Calculated (lines) and measured (markers) IR absorption profiles as a function of CO_2 loading in aqueous (a) MEA, (b) DEA, (c) AMP. The selected wavenumbers are characteristic of free amine (full black line and circles), protonated amine (full gray lines and squares), HCO_3^- (dashed black lines and diamonds), carbamate (dashed gray lines and triangles), CO_3^{2-} (dash-dotted black line and head-down triangles).

The equilibrium constants determined are in good agreement with published values and are given in Table 2 . The formation of the AMP-carbamate species is uncertain with previous studies finding it did not form, or formed to only a small extent (<5% of CO_2 absorbed). In this study, the stability constant K_5 and the estimated pure component spectrum of $AMPCOO^-$ were poorly defined during fitting and did not converge to a consistent minimum value, resulting in a large standard deviation. Fitting log K_5 also slightly perturbed the value of log K_4 while upon its removal log K_4 consistently converged to the same well-defined value.

Table 2. Calculated and Published Equilibrium Constants of Amine Protonation, K_4, and Carbamate Formation, K_5[a]

amine	log K_4	ref	log K_5	ref
MEA	9.06 ± 0.02	9.07,[31] 9.03[32]	1.28 ± 0.02	1.28,[33] 1.31[7]
DEA	8.42 ± 0.03	8.53[34]	0.68 ± 0.02	0.62[34]
AMP	9.64 ± 0.02	9.31,[35] 9.28[32]	not defined	−1.52[36]

[a]The errors for the parameter values are the standard deviations calculated as part of the nonlinear regression algorithm.

The simulated concentrations profiles are displayed in Figure 6. The concentration profiles of the CO_2-MEA system compared well with published values.[37] The amines show different behavior depending upon steric hindrance of the amine group. MEA and DEA show a similar trend, with an increase in the amount of protonated amine and carbamate with CO_2 loading reaching a maximum at 0.5 mol CO_2/mol. The concentration of carbamate then declines as the concentration of bicarbonate increases. For AMP a significant amount of CO_2 is in the carbonate form rather than carbamate. This amount reaches a maximum and then decreases after the CO_2 loading reaches 0.6 mol CO_2/mol.

Carbamate formation, K_5, for AMP was excluded from the equilibrium model. If the formation of $AMPCOO^-$ was simulated using the literature value for the stability constant the amount formed was only 0.6% of the total AMP concentration. If this species is included in the model the stability constant converges to a small value with a large error. Also the estimated pure component spectrum was poorly defined. Together this indicates the value of the stability constant is not defined by the data and excluding carbamate formation is a reasonable assumption.

The fitted value of K_4, the amine protonation constant, is very sensitive to the concentration of amine and CO_2 used in the model. Small changes in concentration can result in significant changes in the value of K_4. For more precise results determination of the total amine concentration and/or CO_2 content via titration would be necessary. Alternatively, the concentration of amine could be fitted as a nonlinear parameter, although this approach was not used here.

The experimental pressure was limited to 7 bar by the ATR-FT-IR immersion probe, restricting the range of possible CO_2 loadings. Measurement at higher CO_2 loading or a number of different amine concentrations would improve the precision of the method as a broader species distribution would be observed. At these higher loadings or different amine concentrations, the mathematical ambiguity between carbamate, protonated amine, and bicarbonate concentrations would be broken. However, at higher loadings, the equilibrium model should also include the protonated carbamate moiety as its concentration may become significant.

■ CONCLUSIONS

In this study, we have successfully demonstrated that CO_2 absorption in MEA, DEA, and AMP aqueous solutions can be qualitatively and quantitatively monitored by *in situ* ATR-FT-IR spectroscopy. Infrared spectra of the CO_2−H_2O−amine system were recorded at equilibrium under different CO_2 loadings. Specific adsorption bands were tentatively assigned to characteristic vibration bands. Because of significant absorption peak overlapping such as bicarbonate and carbamate bands,

dx.doi.org/10.1021/ie302056f | *Ind. Eng. Chem. Res.* 2012, 51, 14317−14324

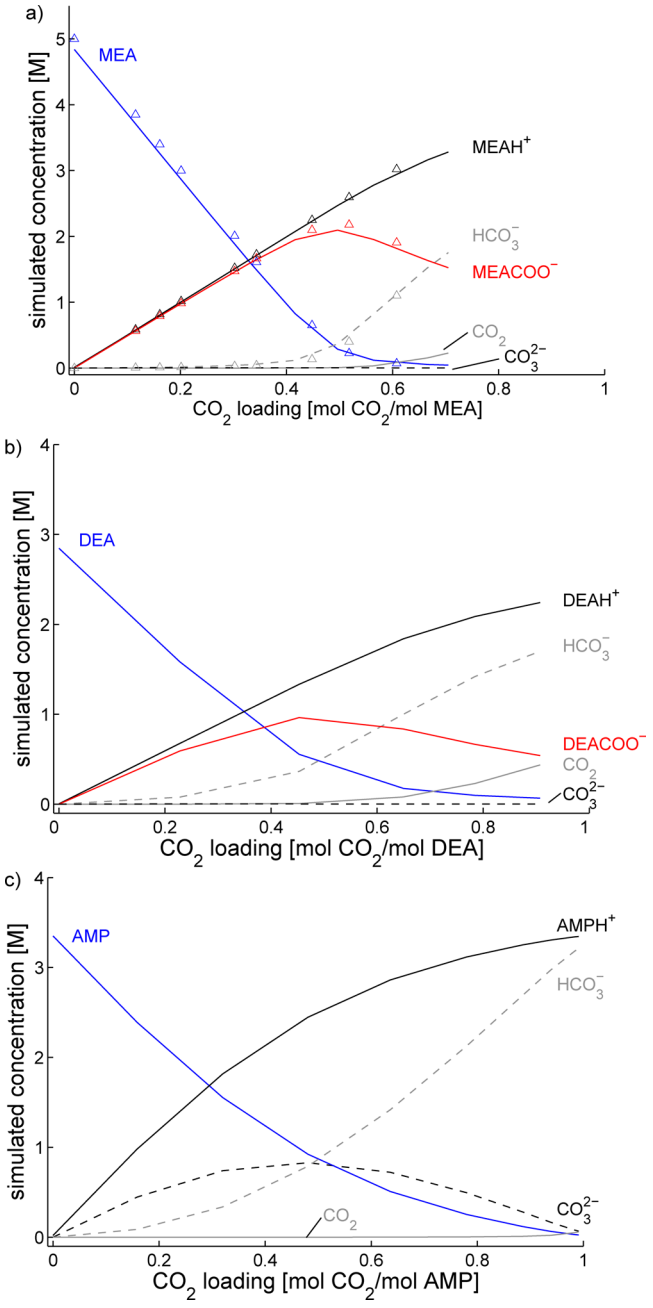

Figure 6. Simulated concentration of MEA (a), DEA (b), and AMP (c) with the equilibrium constants calculated in this study as given in Table 2. For MEA, published values (triangles) extrapolated to 30 wt % MEA are also displayed for comparison.[37]

reference spectra of protonated amine, bicarbonate, and carbonate were recorded. Traditionally, reference spectra are required for determining the species concentration involved during the absorption of CO_2. However for the CO_2–H_2O–amine system straightforward single peak evaluation techniques are intractable due to strong band overlaps. Moreover, carbamate spectra can generally not be calibrated.

As an alternative a calibration-free method based on fitting of a thermodynamic model to multivariate spectroscopic measurements with a nonlinear regression was applied. Carbonate/bicarbonate/CO_2 and water acid–base equilibrium constants were taken from the literature as they are independent of the type of amine investigated. The amine protonation and carbamate equilibrium constants were calculated via the method and agreed well with published data. Simultaneously, speciation of the CO_2–H_2O–amine systems was determined and compared with published equilibrium data.

With primary and secondary amines, mathematical ambiguity due to a close to linear relationship between protonated amine and carbamate concentration required setting the protonated amine as an infrared nonabsorbing species. Working at higher CO_2 loadings or varying the amine concentration would have broken the linear dependence. While this would not change the result it would potentially improve the robustness of the fitted parameter values.

In conclusion, we have demonstrated that CO_2 infrared monitoring can rapidly provide insights into the thermodynamics of CO_2 absorption by aqueous amines. In addition this method could be modified to provide a tool for FT-IR online monitoring of chemical speciation and behavior in an industrial CO_2 capture plant.

AUTHOR INFORMATION

Corresponding Author

*E-mail: gilles.richner@csiro.au.

Notes

The authors declare no competing financial interest.

ACKNOWLEDGMENTS

This project is part of the CSIRO Coal Technology Portfolio. The views expressed herein are not necessarily the views of the Commonwealth, and the Commonwealth does not accept responsibility for any information or advice contained herein.

REFERENCES

(1) Rochelle, G. T. Amine scrubbing for CO_2 capture. *Science* **2009**, *325*, 1652–1654.

(2) Puxty, G.; Rowland, R.; Allport, A.; Yang, Q.; Bown, M.; Burns, R.; Maeder, M.; Attalla, M. Carbon dioxide postcombustion capture: A novel screening study of the carbon dioxide absorption performance of 76 amines. *Environ. Sci. Technol.* **2009**, *43*, 6427–6433.

(3) Porcheron, F.; Gibert, A.; Mougin, P.; Wender, A. High throughput screening of CO_2 solubility in aqueous monoamine solutions. *Environ. Sci. Technol.* **2011**, *45*, 2486–2492.

(4) Böttinger, W.; Maiwald, M.; Hasse, H. Online NMR spectroscopic study of species distribution in MEA–H_2O–CO_2 and DEA–H_2O–CO_2. *Fluid Phase Equilib.* **2008**, *263*, 131–143.

(5) Jakobsen, J. P.; Krane, J.; Svendsen, H. F. Liquid-phase composition determination in CO_2–H_2O–alkanolamine systems: An NMR study. *Ind. Eng. Chem. Res.* **2005**, *44*, 9894–9903.

(6) McCann, N.; Phan, D.; Wang, X.; Conway, W.; Burns, R.; Attalla, M.; Puxty, G.; Maeder, M. Kinetics and mechanism of carbamate formation from CO_2(aq), carbonate species, and monoethanolamine in aqueous solution. *J. Phys. Chem. A* **2009**, *113*, 5022–5029.

(7) Conway, W.; Wang, X.; Fernandes, D.; Burns, R.; Lawrance, G. A.; Puxty, G.; Maeder, M. A comprehensive kinetic and thermodynamic study of the reactions of CO_2(aq) and HCO_3^- with monoethanolamine (MEA) in aqueous solution. *J. Phys. Chem. A* **2011**, *115*, 14340–14349.

(8) Souchon, V.; Aleixo, M. D.; Delpoux, O.; Sagnard, C.; Mougin, P.; Wender, A.; Raynal, L. *In situ* determination of species distribution in alkanolamine–H_2O–CO_2 systems by Raman spectroscopy. *Energy Procedia* **2011**, *4*, 554–561.

(9) Jackson, P.; Robinson, K.; Puxty, G.; Attalla, M. *In situ* Fourier transform-infrared (FT-IR) analysis of carbon dioxide absorption and desorption in amine solutions. *Energy Procedia* **2009**, *1*, 985–994.

(10) Robinson, K.; McCluskey, A.; Attalla, M. I. An FTIR spectroscopic study on the effect of molecular structural variations

on the CO_2 absorption characteristics of heterocyclic amines. *ChemPhysChem* **2011**, *12*, 1088−1099.
(11) Derks, P. W.; Huttenhuis, P. J.; van Aken, C.; Marsman, J.-H.; Versteeg, G. F. Determination of the liquid-phase speciation in the MDEA−H_2O−CO_2 system. *Energy Procedia* **2011**, *4*, 599−605.
(12) Archane, A.; Fürst, W.; Provost, E. Influence of poly(ethylene oxide) 400 (PEG400) on the absorption of CO_2 in diethanolamine (DEA)/H_2O systems. *J. Chem. Eng. Data* **2011**, *56*, 1852−1856.
(13) Geers, L. F. G.; van de Runstraat, A.; Joh, R.; Schneider, R.; Goetheer, E. L. V. Development of an online monitoring method of a CO_2 capture process. *Ind. Eng. Chem. Res.* **2011**, *50*, 9175−9180.
(14) Dyson, R. M.; Jandanklang, P.; Maeder, M.; Mason, C. J.; Whitson, A. New developments for the numerical analysis of spectrophotometric titrations. *Polyhedron* **1999**, *18*, 3227−3232.
(15) Puxty, G.; Maeder, M.; Hungerbühler, K. Tutorial on the fitting of kinetics models to multivariate spectroscopic measurements with non-linear least-squares regression. *Chemom. Intell. Lab. Syst.* **2006**, *81*, 149−164.
(16) Harned, H. S.; Scholes, S. R. The ionization constant of HCO_3^- from 0 to 50°. *J. Am. Chem. Soc.* **1941**, *63*, 1706−1709.
(17) Edwards, T. J.; Maurer, G.; Newman, J.; Prausnitz, J. M. Vapor−liquid equilibria in multicomponent aqueous solutions of volatile weak electrolytes. *AIChE J.* **1978**, *24*, 966−976.
(18) Maeder, M.; Neuhold, Y. M. *Practical Data Analysis in Chemistry*; Elsevier: Amsterdam, 2007.
(19) Puxty, G.; Rowland, R. Modeling CO_2 Mass transfer in amine mixtures: PZ-AMP and PZ-MDEA. *Environ. Sci. Technol.* **2011**, *45*, 2398−2405.
(20) Helgeson, H. C.; Kirkham, D. H.; Flowers, G. C. Theoretical prediction of the thermodynamic behavior of aqueous-electrolytes at high-pressures and temperatures. 4. Calculation of activity-coefficients, osmotic coefficients, and apparent molal and standard and relative partial molal properties to 600°C and 5 kb. *Am. J. Sci.* **1981**, *281*, 1249−1516.
(21) Sipos, P. Application of the specific ion interaction theory (SIT) for the ionic products of aqueous electrolyte solutions of very high concentrations. *J. Mol. Liq.* **2008**, *143*, 13−16.
(22) Peggs, S. L.; Bettin, H. Tables of Physical & Chemical Constants. 2.2.1 Densities. Kaye & Laby Online, version 1.1, http://www.kayelaby.npl.co.uk/ (accessed October 12, 2011), 2008.
(23) Perry, R.; Green, D. *Perry's Chemical Engineers' Handbook*, 7th ed.; McGraw-Hill: New York, 1997.
(24) Silverstein, R.; Bassler, G.; Morrill, T. *Spectrometric Identification of Organic Compounds*, 5th ed.; Wiley: New York, 1991.
(25) Smith, B. C. *Infrared Spectral Interpratation: A Systematic Approach*; CRC Press: Boca Raton, FL, 1999.
(26) Falk, M.; Miller, A. G. Infrared-spectrum of carbon-dioxide in aqueous-solution. *Vib. Spectrosc.* **1992**, *4*, 105−108.
(27) Rudolph, W. W.; Fischer, D.; Irmer, G. Vibrational spectroscopic studies and density functional theory calculations of speciation in the CO_2−water system. *Appl. Spectrosc.* **2006**, *60*, 130−144.
(28) Archane, A.; Gicquel, L.; Provost, E.; Fürst, W. Effect of methanol addition on water−CO_2−diethanolamine system: Influence on CO_2 solubility and on liquid phase speciation. *Chem. Eng. Res. Des.* **2008**, *86*, 592−599.
(29) Cabaniss, S. E.; McVey, I. F. Aqueous infrared carboxylate absorbances: Aliphatic monocarboxylates. *Spectrochim. Acta, Part A* **1995**, *51*, 2385−2395.
(30) Bossa, J. B.; Borget, F.; Duvernay, F.; Theule, P.; Chiavassa, T. Formation of neutral methylcarbamic acid ($CH_3NHCOOH$) and methylammonium methylcarbamate $[CH_3NH_3^+][CH_3NHCO_2^-]$ at low temperature. *J. Phys. Chem. A* **2008**, *112*, 5113−5120.
(31) Bates, R. G.; Pinching, G. D. Acidic dissociation constant and related thermodynamic quantities for monoethanolammonium ion in water from 0 °C to 50 °C. *J. Res. Nat. Bur. Stand.* **1951**, *46*, 349−352.
(32) Fernandes, D.; Conway, W.; Wang, X.; Burns, R.; Lawrance, G.; Maeder, M.; Puxty, G. Protonation constants and thermodynamic properties of amines for post combustion capture of CO_2. *J. Chem. Thermodyn.* **2012**, *51*, 97−102.
(33) Versteeg, G.; van Dijck, L.; van Swaaij, W. On the kinetics between CO_2 and alkanolamines both in aqueous and non-aqueous solutions. An overview. *Chem. Eng. Commun.* **1996**, *144*, 113−158.
(34) Barth, D.; Tondre, C.; Delpuech, J. J. Stopped-flow determination of carbon dioxide-diethanolamine reaction mechanism: Kinetics of carbamate formation. *Int. J. Chem. Kinet.* **1983**, *15*, 1147−1160.
(35) Littel, R. J.; Bos, M.; Knoop, G. J. Dissociation-constants of some alkanolamines at 293-K, 303-K, 318-K, and 333-K. *J. Chem. Eng. Data* **1990**, *35*, 276−277.
(36) Saha, A. K.; Bandyopadhyay, S. S.; Biswas, A. K. Kinetics of absorption of CO_2 into aqueous solutions of 2-amino-2-methyl-1-propanol. *Chem. Eng. Sci.* **1995**, *50*, 3587−3598.
(37) Aboudheir, A.; Tontiwachwuthikul, P.; Chakma, A.; Idem, R. Kinetics of the reactive absorption of carbon dioxide in high CO_2-loaded, concentrated aqueous monoethanolamine solutions. *Chem. Eng. Sci.* **2003**, *58*, 5195−5210.